Thin-Walled Structures 131 (2018) 417–427

Contents lists available at ScienceDirect

Thin-Walled Structures

journal homepage: www.elsevier.com/locate/tws

Full length article

Snap-through buckling of fly ash cenosphere/epoxy syntactic foams under thermal environment

Sunil Waddar, Jeyaraj Pitchaimani*, Mrityunjay Doddamani

Department of Mechanical Engineering, National Institute of Technology Karnataka, Surathkal, India

ARTICLE INFO

Keywords:
Fly ash cenospheres
Syntactic foam
Snap-through buckling
Non-uniform heating

ABSTRACT

Experimental investigation on deflection behaviour of fly ash cenosphere/epoxy syntactic foam at room temperature and under thermal environment (three different heating conditions) is investigated. Influence of fly ash cenosphere volume fraction and nature of temperature variation on deflection behaviour of syntactic foam beam is discussed elaborately. Results reveal that the syntactic foam beam experience snap-through buckling under thermal environment and is reflected by two bifurcation points in temperature-deflection plot. It is observed that the time duration for which the foam beam stays in the first buckled position increases with increase in cenosphere content. Thermal environment induces compressive stresses in the samples causing such snap-through buckling. However, such phenomenon is not observed when mechanical compressive loads are applied under room temperature conditions. Temperature variation across the beam strongly influences snap-through buckling in syntactic foams in addition to volume fraction of filler content.

1. Introduction

In the design process of automobile, aircraft and marine structural components, it is important to investigate their behaviour under thermal loading condition, as weight requirements initiate designers to develop thinner and lighter structures. The development of newer materials necessitates to explore the suitability of thinner structures from stability perspective, as they are prone to undergo static instability [1]. One of the light weight material system which is gaining more popularity due its closed cell structure, built in porosity and higher specific compressive properties is known as syntactic foams. Syntactic foams are prepared by dispersing hollow microballoons in matrix resin resulting in light weight material system having potential weight saving applications. Owing to their higher specific properties, syntactic foam composites are widely used in automotive, marine and aviation sectors [2–5]. Operating conditions of such syntactic foam components in service vary due to mechanical and thermal loads necessitating their investigations under varying temperature conditions.

Existing literature on the temperature dependent properties of the syntactic foams represent coefficient of thermal expansion (CTE), thermal conductivity (TC) and dynamic mechanical analysis (DMA) [6]. Parameters such as volume fraction and wall thickness can be used to tailor these properties effectively. Labella et al. [7] examined CTE of vinyl ester matrix/fly ash and observed 48% decrease in CTE by with increasing filler content from 30 to 60 vol%. In comparison with neat resin, foams exhibited lower CTE values. Li et al. [8] presented numerical investigation of TC in syntactic foams. Their results revealed that TC of foam decrease with increase in microballoons vol%. Numerical investigation by Park et al. [9] revealed that thermal conductivity ratio (ratio of thermal conductivities of microballoon shell to matrix) increases significantly with relative wall thickness of the microballoons at all volume fractions. Effect of volume fraction and wall thickness of hollow glass microballoon (GMB) on thermo mechanical properties of epoxy matrix syntactic foams are studied by Lin et al. [10]. They observed that the CTE of syntactic foams is lower than the neat epoxy due to presence of ceramic particles. The filler volume fraction has a strong effect on the glass transition temperature as compared to wall thickness variations.

Temperature dependent elastic properties of syntactic foam composites have been addressed in Ref's. [11,12]. Gu et al. [13] investigated DMA of fly ash /epoxy syntactic foams and reported that the addition of fly ash enhanced the damping capacity. Studies also revealed that the damping mechanism is governed by matrix viscoelasticity, grain boundary sliding with the cenosphere particles and interfacial sliding friction between the constituents. Similar trend is also observed for modified epoxy and fly ash cenosphere syntactic foams [14]. Hu and Yu [15] investigated thermal, DMA and tensile properties of hollow polymer particle filled in epoxy resin. As compared to neat

* Corresponding author.
E-mail address: pjeyaemkm@gmail.com (J. Pitchaimani).

https://doi.org/10.1016/j.tws.2018.07.013
Received 10 March 2018; Received in revised form 3 July 2018; Accepted 10 July 2018

resin these foams showed higher damping with peaks shifting to higher temperature. Thin-walled structural members with in-plane restrained deflections subjected to thermal environment results in buckling mode failure. Several researchers investigated effect of thermal load on buckling behaviour of structural components having simple geometrical shapes. However, most of the studies are based on analytical [16] and numerical [17–19] approaches with a very less focus on experimental investigations. The influence of nonuniform temperature field on nonlinear buckling behaviour of isotropic beam is investigated through experimental and numerical methods by George et al. [20]. They observed that the critical buckling temperature is strongly influenced by temperature variation conditions. Bhagat and Jeyaraj [21] investigated buckling strength of the aluminium cylindrical panel subjected to nonuniform temperature profiles through experimental approach. Results revealed that the buckling strength significantly varied with location of heating source. These studies bring forth the role of nonuniform temperature profile on the thermal buckling behaviour of the structures and needs to be looked into.

The snap-through buckling of curved beams, shallow arches, cylindrical panels and shells under thermal and mechanical loads has been studied analytically and numerically by several researchers [22–25]. However, experimental investigation on snap-through buckling is scarce. The fundamental mechanisms of snap-through buckling subjected to mechanical load is investigated using shallow arch and a pair of linkages by Wiebe et al. [26]. Dehrouyeh-Semnani et al. [27] examined snap-through buckling behaviour of microbeam made of functionally graded material when subjected to uniform thermal load using numerical method. Wang and Fancey [28] studied bistable morphing of polymeric composite caused due to viscoelastic force induced owing to temperature changes [29]. The snap-through buckling of beam structures subjected to quasi-static loading is analyzed by using elastic theory of prismatic bars by Haung and Vahidi [30]. Chandra et al. [31] combined experimental-computational framework to analyse the snap-through buckling behaviour of clamped-clamped shallow arches subjected to harmonic distributed loadings. Keleshteri et al. [32] investigated snap-through instability of functionally graded carbon nanotube reinforced composite plate with piezoelectric layers. Chandra et al. [33] examined the performance of beam using continuum nonlinear finite element formulations in conjunction with several popular implicit time stepping algorithms to assess the accuracy and stability associated with numerical simulations of snap-through events. Plaut et al. [34] investigated snap-through behaviour of shallow elastic arches under dynamic, unilateral displacement control, with the in dentor moving at constant velocity. Plaut et al. [35] investigated numerically snap-through buckling characteristics of beams and circular arches with the help of unilateral displacement control technique. Liu et al. [36] investigated the stochastic nonlinear snap-through response of a clamped composite panel subjected to the combined severe acoustic excitation and a steady thermal effect using single mode fokker plank distribution function. Studies indicated that the stationary statistical solution of the single-mode analysis captures the features of the displacement density distribution and showed the evolution from no snap-through to a persistent stochastic response. Chen et al. [37] studied the snap-through buckling of a hinged elastica subjected to a midpoint force theoretically and compared the results with experimental observations.

Literature review indicates that the nature of thermal loading influences critical buckling temperature of the structures exposed to elevated temperatures. Similarly, thermal buckling studies on structures made of materials having viscoelastic effect indicate that they are subjected to snap-through buckling. Syntactic foams find applications in marine, automobile and aerospace industries which may be subjected to elevated temperatures during their service resulting from aerodynamic and solar radiation heating. Though wide literature is available fly ash reinforced thermosetting and thermoplastic syntactic foams [38–43], snap-through buckling under thermal environment of these foams are not yet reported to the best of authors knowledge with a focus on interior panels of aircrafts and marine vessels. Cenospheres are varied by 20, 40 and 60 vol% in epoxy matrix and prepared foam samples are subjected to temperature variations in the range of 27–45 °C with three different heating conditions namely, increase-decrease, decrease and decrease-increase along the length of the samples. Effect of filler content and heating conditions on snap-through buckling is presented in this work. Critical buckling temperature is estimated through temperature-deflection plots which are recorded using in-house developed LabVIEW program. Deflection plots of thermal and mechanical loading conditions are compared to discuss the snap-through phenomena. DMA tests are also conducted to understand viscoelastic behaviour of the developed syntactic foams in thermal environment and further to critically analyse snap-through event.

2. Materials and methods

2.1. Constituents materials

LAPOX L-12 epoxy with K-6 room temperature curing hardener (Atul Ltd., Gujarat, India) is used as matrix resin. Cenosphere of CIL 150 grade procured from Cenosphere India Pvt Ltd, Kolkata, West Bengal, India is used as filler. These fly ash cenospheres are spherical in shape and physical, chemical and sieve analysis details in as received condition are available in Ref. [39]. Alumina, silica, calcium and iron oxides are the major constituents of these abundantly available environmental pollutants.

2.2. Syntactic foam preparation

Cenospheres (20, 40 and 60 vol%) and epoxy resin are weighed in a predetermined quantity and stirred slowly until homogenous slurry is formed. Polymerization process is initiated by adding 10 wt% of K6 hardener into the slurry before pouring it into the mold. Subsequently this mixture is decanted into aluminium mold. Silicone releasing agent is applied to the mold for easy confiscation of cast slabs. The castings are allowed to cure for 24 h at room temperature and trimmed using diamond saw to the dimensions of 370 × 12.5 × 4 mm (Fig. 1c). All samples are coded as per nomenclature EXX, where letter 'E' denote neat epoxy resin, 'XX' represents cenosphere volume fraction. Neat resin samples are also prepared under similar processing conditions for comparison.

Experimental densities of all the samples are estimated as per ASTM D792-13. For each composition five samples are tested and the average values with standard deviation are presented in Table 1. Theoretical densities of syntactic foams are calculated using rule of mixtures and is given by,

$$\rho^{th} = \rho_m v_m + \rho_f v_f \tag{1}$$

where ρ and v represent density and volume fraction respectively and suffixes m and f represent matrix and filler respectively. Air entrapped during manual mixing of cenospheres in epoxy resin is represented as void content. Void content (ϕ_v) is calculated by the comparative difference between the theoretical (ρ^{th}) and experimentally measured (ρ^{exp}) density [44] and is given by,

$$\phi_v = \frac{\rho^{th} - \rho^{exp}}{\rho^{th}} \tag{2}$$

Void content estimation is crucial as it compromises the mechanical properties.

2.3. Buckling at room temperature under mechanical loading

Buckling behaviour under mechanical load is carried out with the help of Universal Testing Machine (H75KS, Tinius Olsen make, UK,

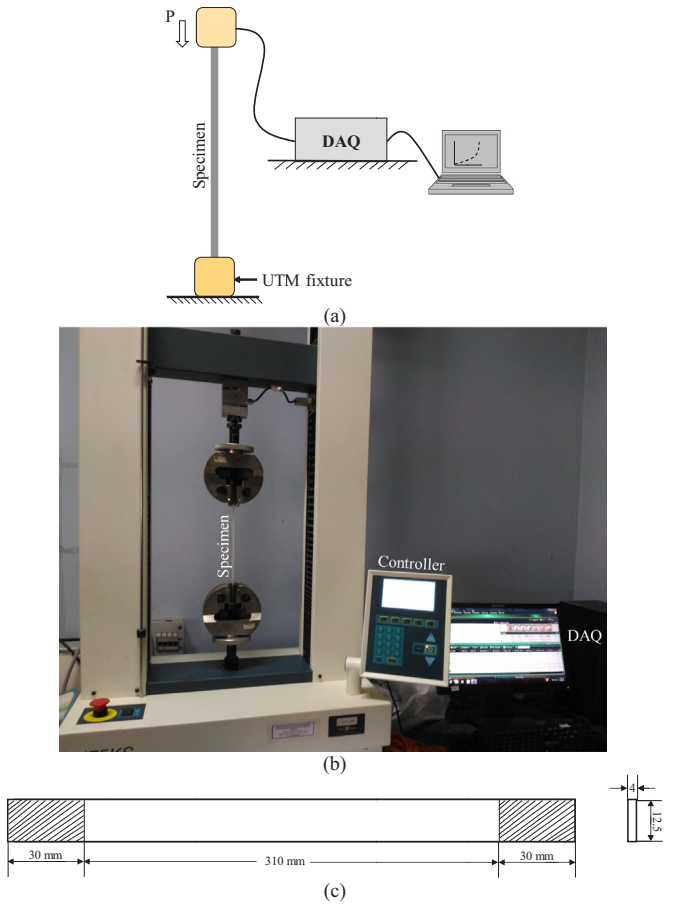

Fig. 1. (a) Schematic representation, (b) actual setup used of estimation of static deflection under mechanical load and (c) Schematic representation of test specimen.

Table 1
Density, void content and weight saving potential of syntactic foams.

Sample Coding	Theoretical density (kg/m^3)	Measured density (kg/m^3)	Matrix void content (%)	% weight reduction w.r.t E0
E0	1189.54	1189.54 ± 0.04	–	–
E20	1135.63	1113.01 ± 3.56	1.99	6.43
E40	1081.72	1057.74 ± 6.48	2.22	11.08
E60	1027.82	1001.49 ± 9.54	2.56	15.81

with load cell capacity of 50 kN). The schematic sketch of the experimental setup is shown in Fig. 1a. Specimens are rigidly clamped at both the ends in the grippers having 310 mm of free length between them to resemble clamped-clamped condition (Fig. 1b). Five specimens of each composition are tested and the average values are reported. Cross-head displacement rate is maintained constant at 0.2 mm/min. The least count of the DAQ used to measure deflection is 0.001 mm. For all tests, the end shortening limit is set at 0.75 mm to explore the behavioural changes, if any, in the post buckling regime.

2.4. Coefficient of thermal expansion (CTE)

The coefficient of thermal expansion is measured as per ASTM D696-13 and the results are utilised to analyse the influence of filler loading in thermal environment. Test temperature is varied from 20 to 90 °C and the corresponding expansion is measured along linear direction using Dilatometer (CIPET, Chennai). Five samples of each composition are tested and the average values are reported.

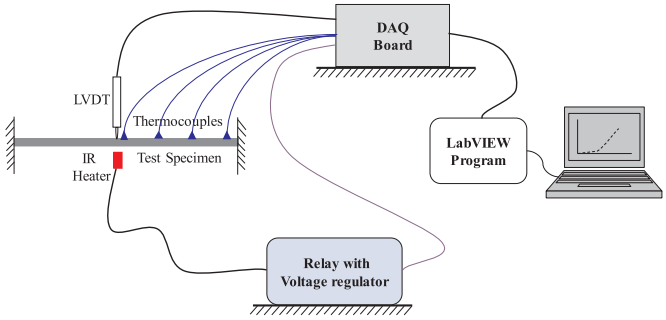

Fig. 2. Schematic representation of buckling setup in thermal environment.

2.5. Buckling under non-uniform thermal load

Fig. 2 shows schematic representation of thermal buckling test setup which is developed in house [20]. Infrared (IR) heaters (1000 W/230 V single tube short wave IR lamps) are used to heat the syntactic foam beams by keeping them at a distance of 30 mm from the lateral surface of the beam. The IR heaters are mounted at different locations along the length of the beam to obtain different non-uniform temperature profiles as shown in Fig. 3. Syntactic foam beams are rigidly clamped at both the ends in a mild steel frame, having 310 mm of free length between them to resemble clamped-clamped boundary condition (Fig. 1c). Further, samples are exposed to thermal load through the radiation heat transfer mode of IR heating source. Linear Variable Differential Transducer (LVDT) of Honeywell MVL7 LVDT make with a stroke length of ± 1 in. having operating temperature range of − 50 °C to + 125 °C is used to measure lateral deflection of beam. Temperature at different locations along the beam length is measured using K-type thermocouples having sensitivity of 41 μV/°C and is recorded in personal

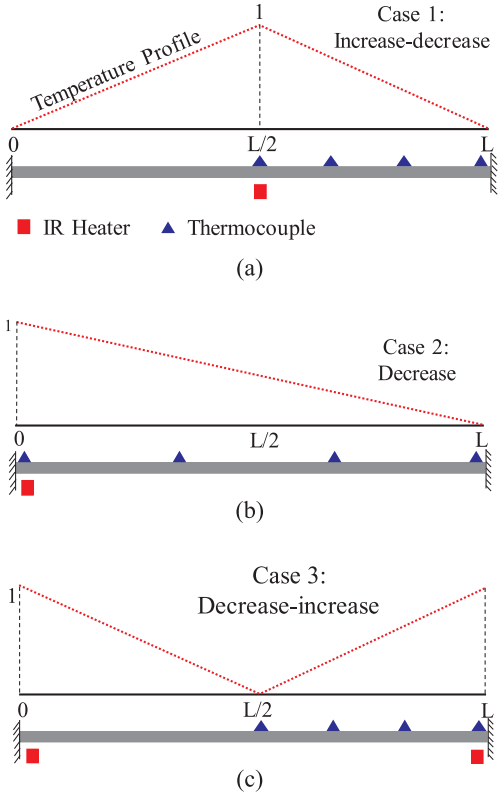

Fig. 3. Schematic representation of (a) Case 1: increase-decrease (b) Case 2: decrease and (c) Case 3: decrease- increase thermal loading conditions.

computer through the data acquisition system (DAQ). A relay unit is used to control ON/OFF state of the IR heater based on the thermocouple output using LabVIEW program which in turn plots temperature-deflection curves.

The maximum measured temperature is fed into the LabVIEW through NI9211 DAQ. Similarly, maximum transverse deflection of the beam is measured using a LVDT and noted through NI9215 DAQ. Temperature on the specimen is increased using IR heater. The entire experimentation is computer controlled using LabVIEW user interface. The temperature and deflection data are stored using shift registers into an array to graph the temperature-deflection plots. The maximum desired temperature up to which the specimens needs to be heated is given as a user input to LabVIEW based on the preliminary experiments conducted for estimating critical buckling temperatures. These recorded temperature values are used as maximum temperature to be attained in the experiments. This procedure is repeated for all the samples prepared. Among all the recorded temperature values for all the syntactic foams including neat epoxy samples, maximum temperature is noted for E60 and is set for IR heater (desired temperature). A comparison is made between the desired and thermocouple temperature. Based on the binary output from the comparison, a case structure is used to switch the NI9481 DAQ which decides ON/OFF state of the IR heater. With the help of statistics palette, the rms value of the LVDT data obtained from the NI9215 DAQ is extracted before forming the array of temperature-deflection data to be used to plot the curves. All data points are merged into a Microsoft excel file using write command.

Three different types of temperature conditions (Case 1, Case 2 and Case 3) are considered by keeping the IR heaters in different locations as shown in Fig. 3. Increase-decrease heating (Case 1) is carried out by placing IR heater at beam center as shown in Fig. 3a. In this case the maximum temperature load is at the midpoint of the beam. Fig. 3b represents Case 2 (decrease heating) wherein IR heater is located at left end of the beam subjecting it to the higher temperature at one end and the lower temperature at the other end. In case 3 of decrease-increase condition, IR heaters are placed at either beam ends and thereby maximum temperature load is applied at the both ends of the beam as presented in Fig. 3c. These three cases represent broad spectrum of non-uniform thermal loading which may resemble practical in-service conditions.

2.6. Dynamic mechanical analysis (DMA)

Temperature dependent properties of the neat epoxy and their syntactic foams are analyzed using DMA 8000 (Perkin Elmer) within the temperature range of 27–180 °C with incremental temperature of 5 °C in dual cantilever mode replicating clamped-clamped boundary condition. Understanding viscoelastic behaviour of the samples is important from temperature-deflection perspective in order to analyse snap-through buckling phenomena.

3. Results and discussions

3.1. Material processing

Fig. 4 presents micrographs of cenospheres and representative syntactic foam. Fly ash cenospheres are used in as received condition i.e. without any surface modifications. Interfacial bonding strength between the constituents governs tensile and flexural properties as

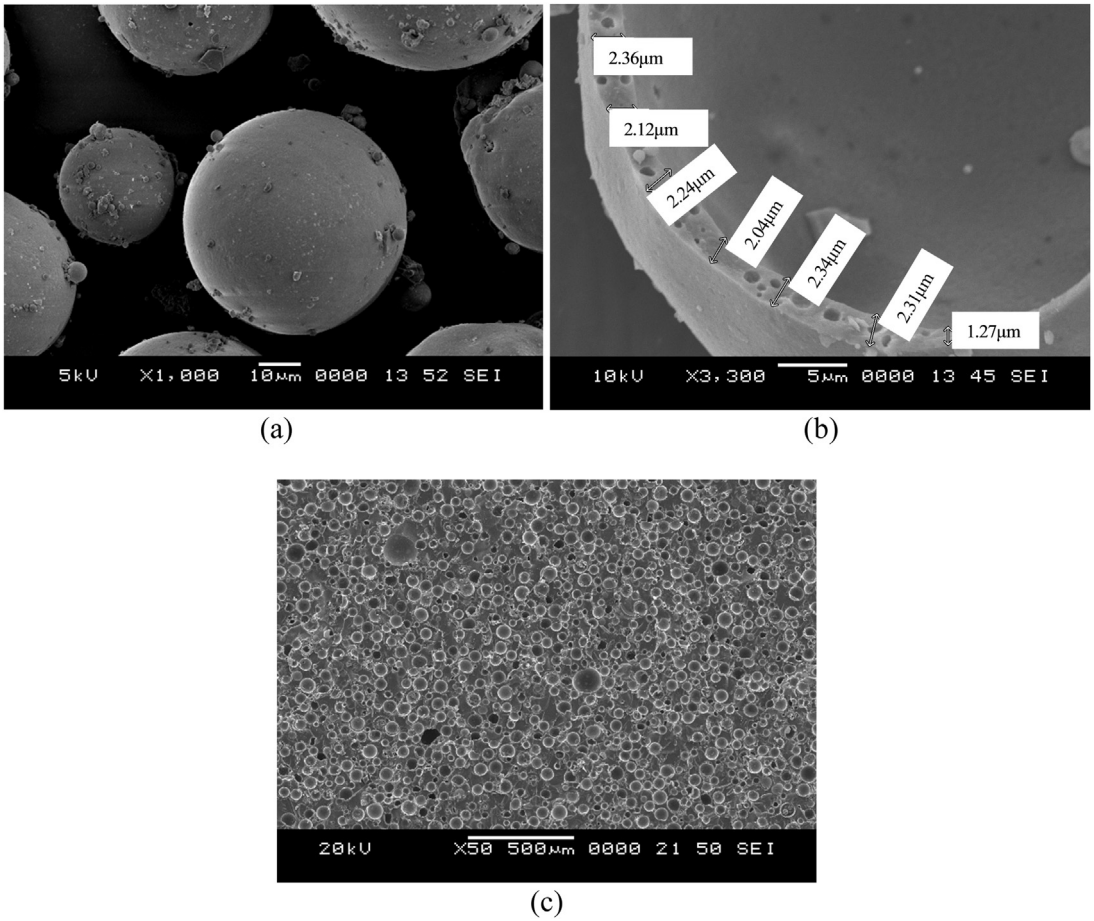

Fig. 4. Micrographs of (a) cenosphere particles (b) wall thickness variations and in-built porosity present in cenospheres and (c) representative E60 syntactic foam at lower magnification showing uniform dispersion of particles in matrix resin.

cracks in interfacial region forms under these conditions [40,41]. However, mechanical properties are less sensitive to interfacial adhesion in compression [45,46]. Further, comparison of mechanical properties with non-uniform coating layer becomes quite challenging [44] and is beyond the scope of the present work.

Micrograph of as received cenospheres is presented in Fig. 4a. Sphericity variations and presence of numerous defects on cenospheres leads to non-uniform surface morphology. Higher magnification of one such broken cenosphere (Fig. 4b) depicts wall thickness variations and in-build porosity within the shell. Deviation between experimental and empirical and/or mathematical models is due to such variations. Particle size analysis of cenospheres reveal that the volume weighted mean particle size is 55 μm [47]. Density of cenospheres is measured to be 0.92 g/cc [39]. Sphericity range of 0.6–0.85 is observed for these fly ash cenosphere particles [40]. Surface defects as observed from Fig. 4a leads to deviation from '1', a perfectly spherical particle. Sound quality of the developed syntactic foams during processing depends upon minimum particle failure, lower cluster formation and uniform dispersion of cenospheres in the matrix resin. In the present work manual stirring approach is adopted to fabricate cenosphere/epoxy syntactic foams. Fig. 4c presents low magnification micrograph of as cast representative E60 sample. Cenospheres are uniformly distributed in the epoxy resin as seen from this micrograph demonstrating the feasibility of the methodology adopted in the present work to prepare the foam samples. As anticipated from Fig. 4c clusters are not seen to be formed in the E60 foam. Quantification of void content and cenosphere survival is crucial as it affects quality and mechanical behaviour of the samples.

Density and void content results are presented in Table 1. Eq. (1) is used to estimate theoretical density which is noted to be higher as compared to experimental value (Table 1). Mechanical mixing of cenospheres in the epoxy resin causes air entrapment in matrix resulting in lower experimental density values as compared to the theoretical ones. Few entrapped air pockets as seen from Fig. 4c is also observed in the representative E60 sample which is a typical feature of syntactic foams. These air pockets are referred as voids and are undesirable from mechanical properties perspective. Eq. (2) is used to compute void content present in all the samples and average values of five replicates across each foam configuration are presented in Table 1. Void content increases with increase in filler loading and is observed to be lower than 2.56%. Such a low value signifies good quality of prepared samples. Density of all the foams decrease (6.43–15.81%) with increasing cenosphere content due to higher amount of hollow microballoons in the matrix resin. Standard deviations vary in a narrow range confirming consistency in syntactic foam processing. Furthermore, Table 1 also reports weight saving potential by comparing foam densities with neat resin. Highest weight saving potential of 15.81% is observed for E60. Exploiting these lightweight syntactic foams for automobile, aerospace and marine applications owing to higher specific mechanical properties in particular under buckling scenario are worth investigating.

3.2. Buckling under mechanical load

Static transverse deflection of the cenosphere/epoxy syntactic foam beam under axial mechanical compressive load is investigated initially. Sample is mounted with clamped-clamped boundary condition in universal testing machine and the axial compressive load is applied as mentioned earlier. For all the tested samples the maximum deflection is seen to be occurring at the beam mid-point (length wise). Test is terminated when beam deflection is seen to be increasing at constant load (region *b–c* in Fig. 5). Slope change in the curves of the samples presented in Fig. 5 indicate critical buckling load. Except for E60, slope change can be located easily. In case of E60, non-linearity creeps in during the slope change. This might be due to constrained matrix flow around higher content of cenospheres present at higher filler loading. Buckling load increases with increasing filler content. With higher

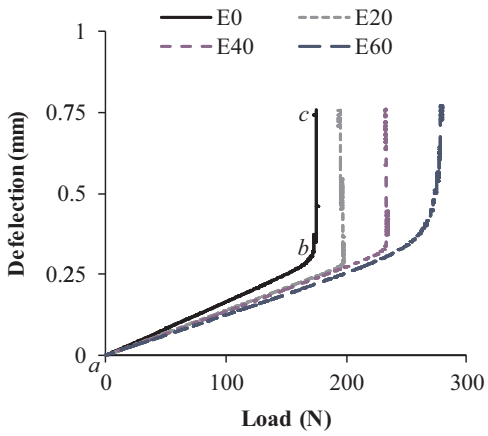

Fig. 5. Deflection of neat epoxy and their syntactic foams under mechanical loads.

cenosphere content, load-deflection plot shifts towards right side implying higher load bearing capabilities of these cenosphere/epoxy syntactic foams under buckling mode. This can be attributed to addition of stiff hollow cenospheres in epoxy matrix which enhances overall stiffness of the composite. All the samples are seen to be regaining the original shape in post-test (Fig. 6c) scenarios as like in pre-test (Fig. 6a) without any significant indication of plastic/permanent deformation. Fig. 6b shows buckled shape of syntactic foam specimen during the test. Under thermal environment it would be interesting to see the influence of heating conditions on deflection behaviour of cenosphere/epoxy syntactic foams and if they can retain their original shape post-test. Coefficient of thermal expansion of all the samples needs to be looked into carefully in analysing thermal environment effect on these foams.

3.3. Coefficient of thermal expansion (CTE)

CTE of neat epoxy and their syntactic foams is presented in Table 2.

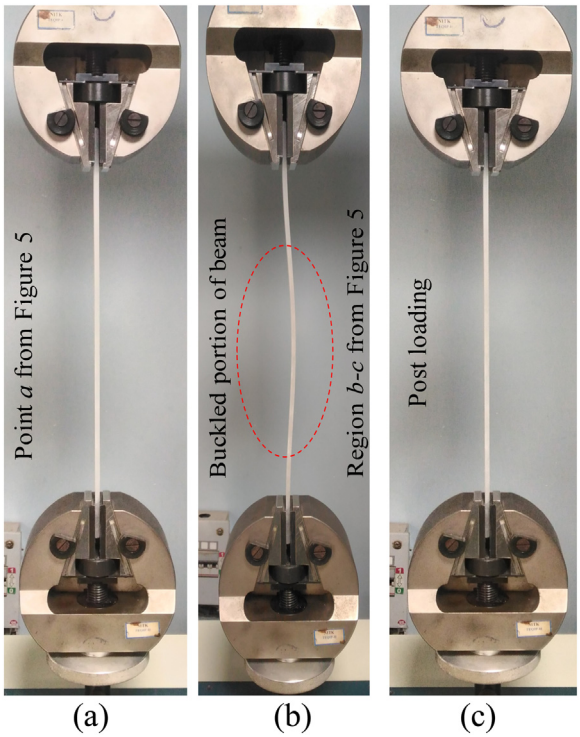

Fig. 6. Test in-progress for representative foam sample (a) pre (b) during and (c) post loading conditions.

Table 2
CTE of neat epoxy and their syntactic foams.

Sample coding	CTE × 10^{-6} (/°C)	% reduction w.r.t E0
E0	82.03 ± 1.76	–
E20	70.61 ± 1.54	13.92
E40	48.84 ± 1.19	40.46
E60	41.88 ± 0.83	48.95

It is observed that CTE of foams reduces significantly with increase in cenosphere content. Such an observation can be attributed to difference in thermal conduction between epoxy resin, cenosphere shell and the gas present within the cenosphere [7]. CTE of cenosphere/epoxy syntactic foams decreases in the range of 13.92–48.95% with increasing filler content as compared to neat epoxy. Fig. 7 shows the mechanism in which heat transfer takes place in neat epoxy and syntactic foams. The heat transfer in neat epoxy samples is mainly influenced by thermal conduction (Fig. 7a), whereas in syntactic foam samples it is influenced by thermal conduction (red color arrows) between epoxy matrix and exterior surface of the cenospheres and vice-versa and thermal convection (blue color arrows) between gas molecules present within the cenospheres (Fig. 7b). With increasing cenospheres content, heat transmission through the syntactic foam becomes increasingly tough and poses higher resistance for heat flow reducing thermal expansion to a greater extent. Further, presence of low CTE elements like Al_2O_3 and SiO_2 as primary constituents in fly ash cenospheres [7], lowers CTE values for foams at highest filler loading.

3.4. Deflection behaviour under mechanical and thermal loading

Deflection behaviour of E0 and E20 samples under room temperature and at different heating conditions are carried out initially. Fig. 8 shows deflection pattern of the samples subjected to mechanical (room temperature condition) and thermal loads. It is observed from the experiments that the beams undergo typical deflection behaviour when subjected to mechanical axial compression (Fig. 8a) and seen to be absent in non-uniform increase-decrease thermal environment (Fig. 8b). It is also observed that the beams undergo different deflection pattern in thermal environment as compared to mechanical loading. Different pattern is clearly evident from Fig. 8b for E0 and E20 samples. In order to understand this behaviour temperature-deflection plot associated with E20 under Case 1 is presented in Fig. 9. Cenosphere/epoxy syntactic foam samples undergo four changes in the trend.

(I) Initial rapid deflections in negative direction (negative values in Y axis) for the small amount of temperature rise (*a–b*).
(II) No significant change in deflection behaviour for further rise in temperature (*b–c*), i.e. the beam stays with a particular geometrical shape (buckled shape) occurred at the end of step I. This can be attributed to the energy gain i.e storage of energy till the beam gets snap initiation.
(III) With further increase in temperature, syntactic foam beam starts to deflect in opposite direction (towards zero deflection - positive Y axis) and passes through the initial position (*c–d*).
(IV) Sample continues to undergo deflection exponentially (*d–e*) with temperature rise and experiences same kind of geometrical shape change as exhibited in step II but in opposite direction. This clearly indicates that the syntactic foam beam undergoes “snap-through” type of buckling under thermal environment. However, the same beam when subjected to mechanical (room temperature) compression, snaps-through behaviour is absent. This clearly indicates that viscoelastic behaviour creeped in due to temperature rise leads to different temperature-deflection response of syntactic foam composite. The intersection of the tangents drawn at regions *a–b* and *b–c* is considered as first bifurcation point and is represented as T_{cr_1} where as T_{cr_2} is the second bifurcation point at the intersection of tangents drawn to *b–c* and *c–e* regions [20,48]. These are two critical buckling temperatures representing first buckling mode and snap-through buckling initiation point respectively. E20 shows presence of both T_{cr_1} and T_{cr_2} as against T_{cr_1} in E0. The entirely different deflection behaviour of the beam under thermal load is due to the temperature dependent viscoelastic effect of the syntactic foam. This observation clearly indicated influence of cenospheres contributing towards snap-through phenomena. Influence of filler loading and heating conditions on extent of T_{cr} values needs to be explored further.

3.5. Buckling under non-uniform thermal load

All the samples are subjected to three different non-uniform heating conditions as shown in Fig. 3. Maximum temperature associated with each heating condition for all the samples are recorded to plot temperature-deflection response. Deflection is measured at the mid-point (length wise) since the samples are expected to deflect in the first bending mode. Deflection variation of neat resin and their syntactic foam composites as a function of temperature under different heating conditions is depicted by Fig. 10. Fig. 9 presents all the terminologies used pertaining to four trend changes as discussed in Section 3.4. Deflection of syntactic foam composites reduces with increase in filler content in regions *a–b*, *b–c* and *c–d*. This can be attributed to increase in storage modulus of the syntactic foam with increase in volume fraction of fly ash cenospheres [49,50]. Temperature range for which the syntactic foam remains in buckled shape (*b–c* region) increases with increase in cenosphere content (Fig. 10). With increase in temperature, significant amount of viscoelastic forces develops in foams. This time-dependent phenomenon keeps the beam in the same buckled shape (*b–c*

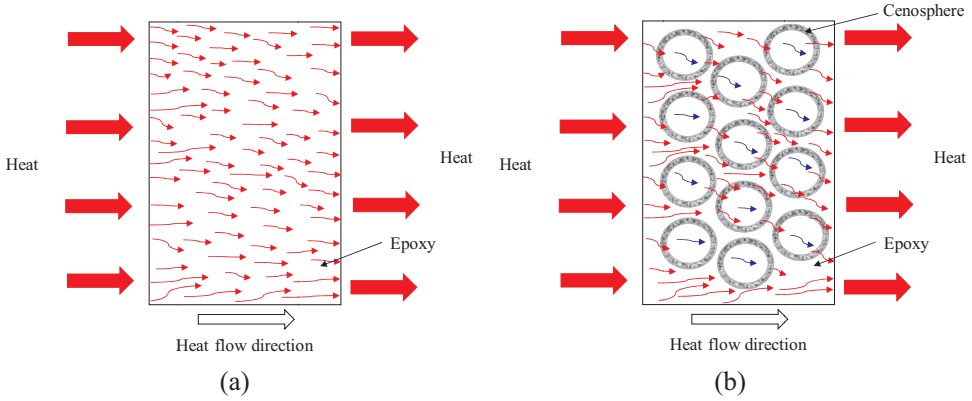

Fig. 7. Heat flow mechanism in (a) neat epoxy and (b) syntactic foam (red arrows indicate conduction and blue arrows indicate convection mode of heat transfer).

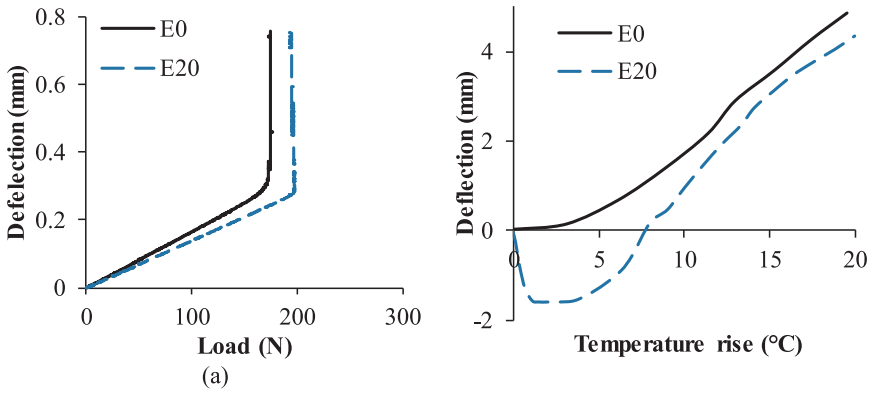

Fig. 8. Behaviour of E20 syntactic foams under (a) mechanical and (b) thermal load.

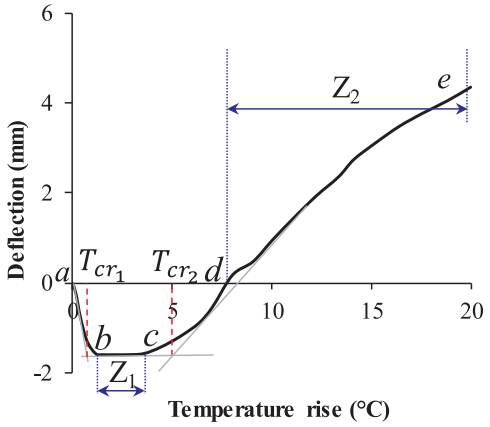

Fig. 9. Estimation of buckling temperature from the temperature-deflection plot for representative E20 sample.

region) for a particular period of time with temperature rise. With further increase in temperature, the buckled beam (Z_1 as seen in Fig. 9) deforms in opposite direction until it attains buckled geometry Z_2. This trend is observed for all the syntactic foams subjected to all the three different heating conditions.

Fig. 11 represent temperature-deflection curves for neat resin and their syntactic foam beams subjected to various thermal loading conditions (Fig. 3). From Fig. 11, it is observed that the deflection behaviour under increase-decrease and decrease-increase heating conditions are similar. It is also observed that deflection under increase-decrease heating is higher than decrease-increase heating which can be attributed to the location of heating source. In the case of increase-decrease heating the source is located at the center of the beam where the stiffness of the beam is very less, hence the deflection is more. However, deflection behaviour under decrease heating is different from other two cases due to unsymmetrical temperature distribution. In non-uniform heating of structures, the deflection and critical buckling temperature is pronounced by amount of beam portion exposed to highest temperature of a particular temperature profile and location of heat source. During decrease heating (Fig. 3b), the beam is exposed to higher temperature at one of its constrained end and the rate of reduction in structural stiffness is less as compared other heating conditions thereby resulting in lower deflection values. In the case of increase-decrease heating (Fig. 3a), the intensity of heat is high at the mid-point of the beam hence the beam experiences higher deflection. In decrease-increase heating (Fig. 3c), the intensity of heat is more at both the ends and rate of reduction in structural stiffness is not higher as compared to increase-decrease heating case and thereby deflections are lower than the increase-decrease case. The temperatures at which neat epoxy and their syntactic foams showed buckled geometrics (due to snap-through action) are presented in Table 3. The buckling temperature is maximum for decrease heating condition and minimum for increase-decrease heating condition. The decrease-increase heating condition has intermediate temperature than the other two heating conditions. Fig. 12 show progressive images of syntactic foam beam undergoing snap through deflection with increase in temperature. Initially the beam undergoes sudden deflection without much increase in temperature ($\leq$ 2 °C) form the reference temperature (27 °C). Fig. 13a show test specimen before application of thermal load and Fig. 13b shows buckled shape of syntactic foam specimen after the test indication plastic/permanent deflection. In order to understand the reason behind the sudden deflection with temperature rise, viscoelastic characteristics of the syntactic foams are presented next.

With increase in cenosphere content the storage modulus of the syntactic foam increases. As a result of this, the period in which the beam stays in *b*–*c* region (stage II) increases with filler content. The restoring force is very less for neat resin samples and hence does not undergo deformation stages as observed in syntactic foams. Fig. 14a represents influence of cenosphere volume fraction on storage modulus of syntactic foams. Storage modulus of neat epoxy resin decreases continuously from room temperature indicating reduction in energy storing capability with temperature rise. Enhancement of storage modulus (with a conceptual correspondence to stiffness) is seen with increasing filler content. Storage modulus of the syntactic foams when compared with room temperature values, slight increase in storage modulus values is noted from 27 to 32 °C followed by decrease thereafter (Fig. 14a). This observation clearly indicates syntactic foams have better energy storing capability at the initial rise in temperature (until 32 °C) as compared to neat resin. This energy storing ability increases with fly ash cenosphere content. This can be attributed to less molecular motions of epoxy molecules owing to cenosphere addition making foam samples to stays in region *b*–*c* for longer duration.

Loss modulus represents dissipation of energy. It is observed from Fig. 14b that loss modulus of epoxy resin is higher than that of syntactic foams in temperature range of 27–45 °C. It can be attributed to less internal sliding between the molecules of epoxy and between the particles and matrix. The effect of matrix viscoelasticity is more and the frictional energy dissipation is relatively low at lower filler loadings. At the higher filler contents, the contribution of matrix viscoelasticity reduces due to intense dilution of cenosphere particles in the epoxy resin. At the same time the intra molecular motion of the matrix becomes difficult that hinders the frictional energy dissipation of chain segments and thereby reduces the heating loss. Syntactic foams exhibited higher storage modulus and lower loss modulus as compared to neat resin.

Cenosphere/epoxy syntactic foams developed in this study exhibited snap-through buckling in thermal environment making them potentially viable light weight material system in aerospace, automobile, marine and other structural engineering applications.

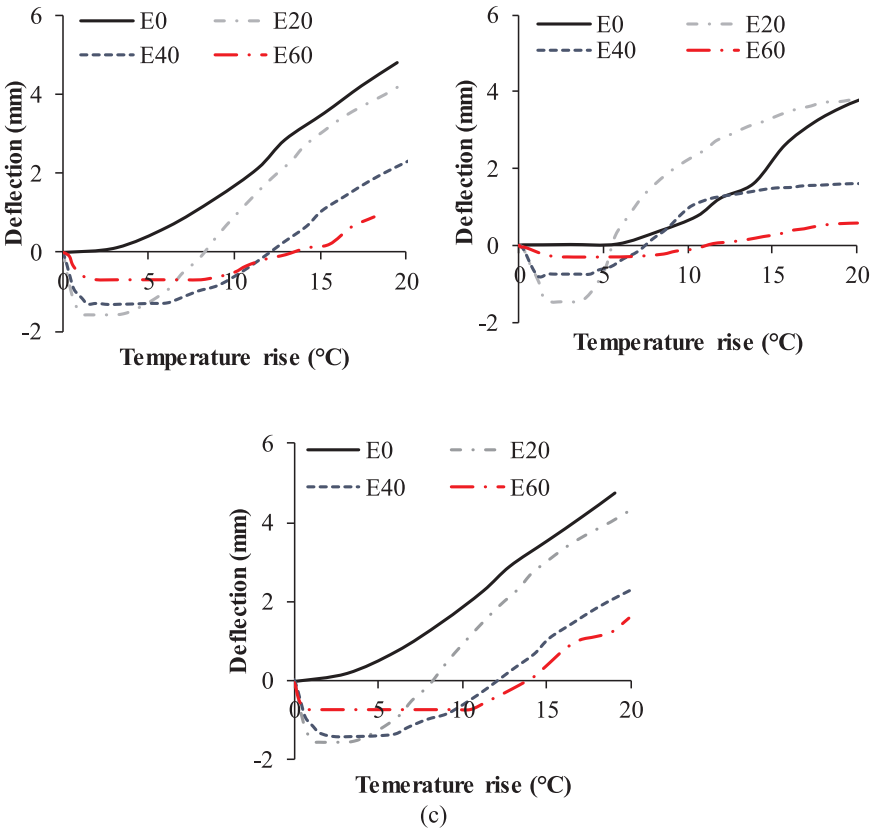

Fig. 10. Influence of cenosphere loading on (a) Case 1: Increase-decrease (b) Case 2: Decrease and (c) Case 3: Decrease-increase heating conditions.

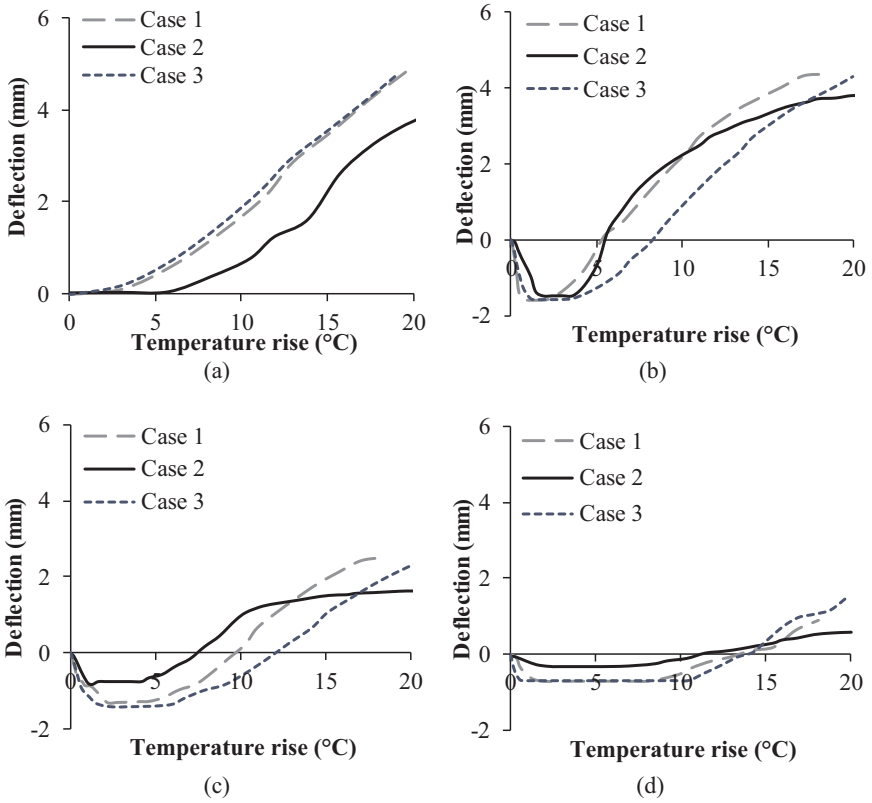

Fig. 11. Influence of temperature variation on (a) E0 (b) E20 (c) E40 and (d) E60 samples.

Table 3
Deflection temperatures for neat epoxy and syntactic foams at various non-uniform heating conditions.

Sample coding	Case 1 Increase-decrease		Case 2 Decrease		Case 3 Decrease-increase	
	T_{cr_1} (°C)	T_{cr_2} (°C)	T_{cr_1} (°C)	T_{cr_2} (°C)	T_{cr_1} (°C)	T_{cr_2} (°C)
E0	4.43 ± 0.25	–	6.45 ± 0.35	–	4.45 ± 0.07	–
E20	0.60 ± 0.14	4.50 ± 1.41	1.38 ± 0.18	7.57 ± 0.04	0.80 ± 0.14	4.45 ± 0.78
E40	0.88 ± 0.04	7.60 ± 1.13	0.90 ± 0.14	10.10 ± 0.42	0.95 ± 0.21	6.23 ± 1.03
E60	0.90 ± 0.42	9.15 ± 0.49	1.30 ± 0.57	12.50 ± 1.41	0.55 ± 0.07	11.25 ± 0.07

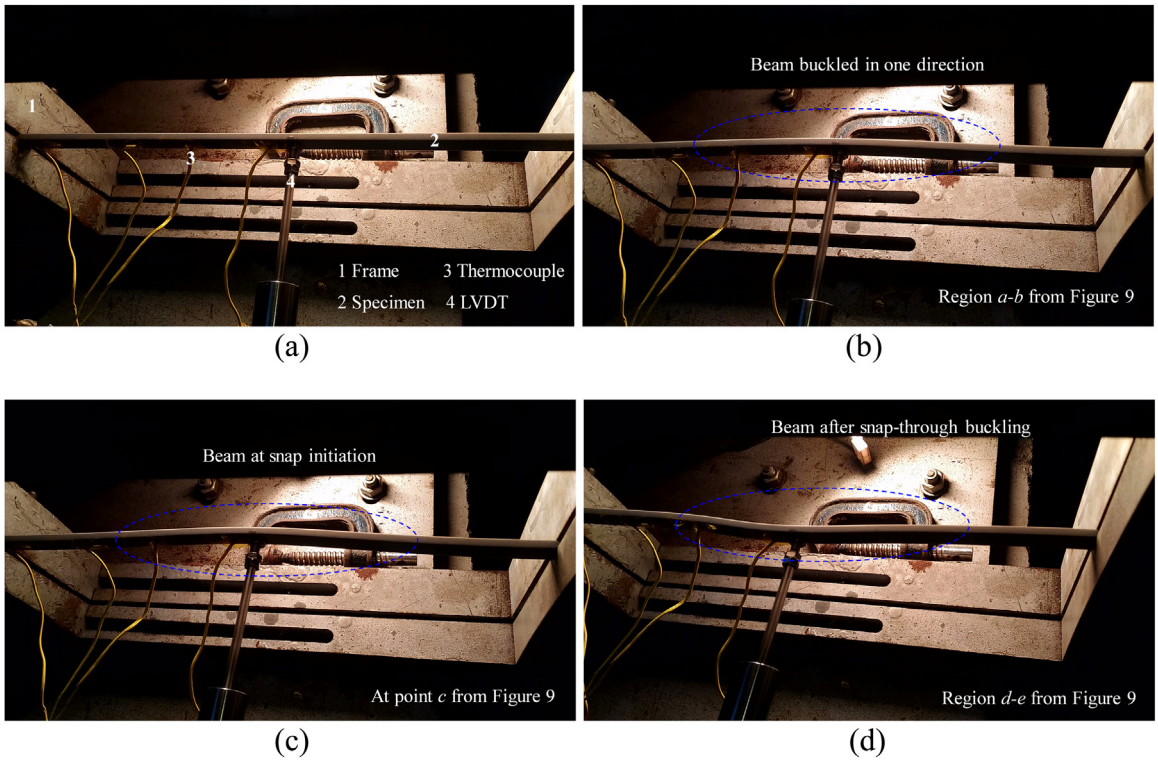

Fig. 12. Progressive images of syntactic foam beam deflecting under increase-decrease heating condition.

4. Conclusions

Deflection behaviour of fly ash cenosphere/epoxy syntactic foams at room temperature (mechanical load) and under thermal environment (three different heating conditions) is presented in this study and following conclusions are drawn:

- Micrographs of as cast sample show uniform distribution of cenospheres in epoxy matrix resin and no signs of cluster formation.
- Density of syntactic foams decrease with increasing cenosphere content and becomes 15.81% lower for syntactic foam containing 60 vol% of cenospheres as compared to neat epoxy resin.
- Void content increases in narrow range of ≤ 2.56% with increase in cenosphere loading in epoxy resin, signifying good quality of fabricated samples.
- Samples subjected to mechanical axial compression at room

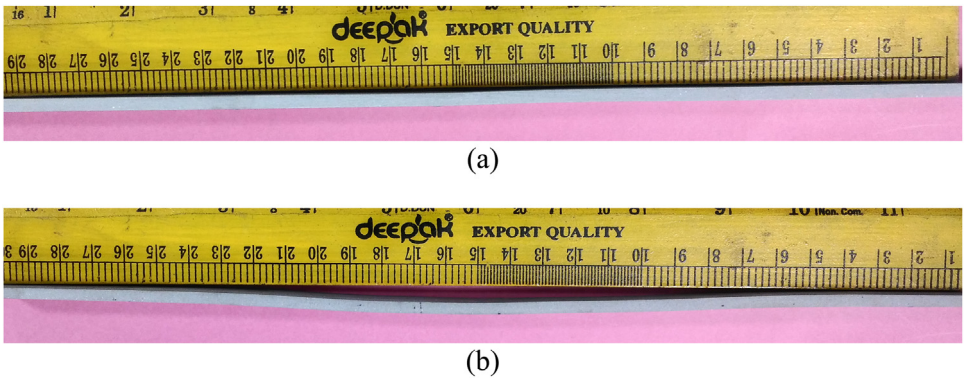

Fig. 13. Representative foam sample (a) pre-buckling (c) post thermal buckling.

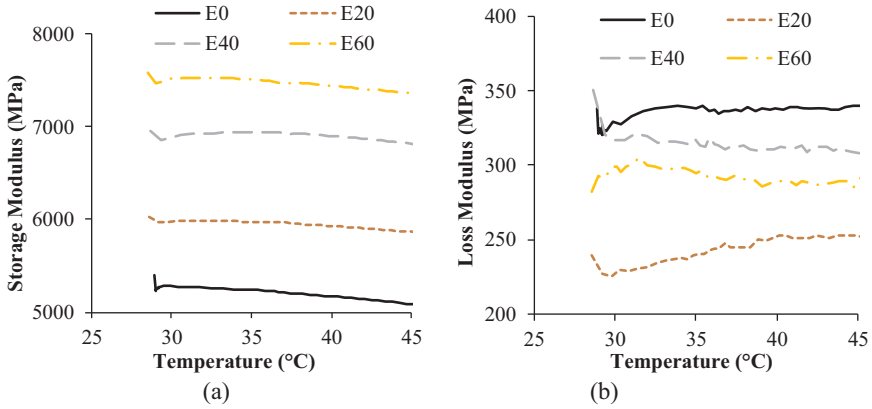

Fig. 14. Influence of cenosphere volume fraction on (a) storage and (b) loss modulus of syntactic foams.

temperature show increase in buckling load in range of 14.42–59.01% for increase in cenosphere content from 20 to 60 vol % as compared to neat epoxy resin.

- All samples subjected to mechanical axial compressive loads, regained to its original shape after the test, without any indication of plastic/permanent deformation.
- CTE of cenosphere/epoxy syntactic foams decreases in the range of 13.92–48.95% with increasing filler content as compared to neat epoxy resin.
- All the samples are subjected to three different non-uniform heating conditions and the temperature-deflection curves reveal that the syntactic foams undergo snap-through buckling behaviour.
- The deflection of syntactic foams reduces with increase in cenosphere content.
- Temperature range for which the syntactic foam remains in initial buckled shape increases with increase in cenosphere content.
- Decrease heating condition show higher buckling temperatures as compared to other two heating cases.
- Dynamic mechanical analysis of cenosphere/epoxy syntactic foams show that the foams have better energy absorbing capability than neat epoxy resin.

Acknowledgments

The authors thank the Department of Mechanical Engineering at National Institute of Technology Karnataka for providing facilities and support.

References

[1] K.D. Murphy, D. Ferreira, Thermal buckling of rectangular plates, Int. J. Solids Struct. 38 (22) (2001) 3979–3994.
[2] N. Gupta, S.E. Zeltmann, V.C. Shunmugasamy, D. Pinisetty, Applications of polymer matrix syntactic foams, JOM 66 (2) (2014) 245–254.
[3] M.L. Jayavardhan, B.R. Bharath Kumar, M. Doddamani, A.K. Singh, S.E. Zeltmann, N. Gupta, Development of glass microballoon/HDPE syntactic foams by compression molding, Compos. Part B: Eng. 130 (2017) 119–131.
[4] M.R. Doddamani, S.M. Kulkarni, Kishore, Behavior of sandwich beams with functionally graded rubber core in three point bending, Polym. Compos. 32 (10) (2011) 1541–1551.
[5] M.L. Jayavardhan, M. Doddamani, Quasi-static compressive response of compression molded glass microballoon/HDPE syntactic foam, Compos. Part B: Eng. 149 (2018) 165–177.
[6] N. Gupta, S.E. Zeltmann, D.D. Luong, M. Doddamani, Testing of foams, in: S. Schmauder, et al. (Ed.), Handbook of Mechanics of Materials, Springer Singapore, Singapore, 2018, pp. 1–40.
[7] M. Labella, S.E. Zeltmann, V.C. Shunmugasamy, N. Gupta, P.K. Rohatgi, Mechanical and thermal properties of fly ash/vinyl ester syntactic foams, Fuel 121 (Suppl. C) (2014) S240–S249.
[8] X. Li, B. Yu, P. Wang, X. Zhang, T. Fan, J. Yang, Unit cells for thermal analyses of syntactic foams with imperfect interfaces, Compos. Commun. 3 (Suppl. C) (2017) S28–S32.
[9] Y.K. Park, J.-G. Kim, J.-K. Lee, Prediction of thermal conductivity of composites with spherical microballoons, Mater. Trans. 49 (12) (2008) 2781–2785.
[10] T.C. Lin, N. Gupta, A. Talalayev, Thermoanalytical characterization of epoxy matrix-glass microballoon syntactic foams, J. Mater. Sci. 44 (6) (2009) 1520–1527.
[11] N. Gupta, D. Pinisetty, A review of thermal conductivity of polymer matrix syntactic foams—effect of hollow particle wall thickness and volume fraction, JOM 65 (2) (2013) 234–245.
[12] S. Sankaran, K.R. Sekhar, G. Raju, M.N.J. Kumar, Characterization of epoxy syntactic foams by dynamic mechanical analysis, J. Mater. Sci. 41 (13) (2006) 4041–4046.
[13] J. Gu, G. Wu, Q. Zhang, Preparation and damping properties of fly ash filled epoxy composites, Mater. Sci. Eng.: A 452–453 (Suppl. C) (2007) S614–S618.
[14] J. Gu, G. Wu, Q. Zhang, Effect of porosity on the damping properties of modified epoxy composites filled with fly ash, Scr. Mater. 57 (6) (2007) 529–532.
[15] G. Hu, D. Yu, Tensile, thermal and dynamic mechanical properties of hollow polymer particle-filled epoxy syntactic foam, Mater. Sci. Eng.: A 528 (15) (2011) 5177–5183.
[16] Y. Fu, J. Wang, S. Hu, Analytical solutions of thermal buckling and postbuckling of symmetric laminated composite beams with various boundary conditions, Acta Mech. 225 (1) (2014) 13–29.
[17] P. Jeyaraj, Buckling and free vibration behavior of an isotropic plate under non-uniform thermal load, Int. J. Struct. Stab. Dyn. 13 (03) (2013) 1250071.
[18] J. Li, Y. Narita, Z. Wang, The effects of non-uniform temperature distribution and locally distributed anisotropic properties on thermal buckling of laminated panels, Compos. Struct. 119 (Suppl. C) (2015) S610–S619.
[19] H.-S. Shen, Y. Xiang, F. Lin, Thermal buckling and postbuckling of functionally graded graphene-reinforced composite laminated plates resting on elastic foundations, Thin-Walled Struct. 118 (2017) 229–237.
[20] N. George, P. Jeyaraj, S.M. Murigendrappa, Buckling of non-uniformly heated isotropic beam: experimental and theoretical investigations, Thin-Walled Struct. 108 (Suppl. C) (2016) S245–S255.
[21] V. Bhagat, J. P, Experimental investigation on buckling strength of cylindrical panel: Effect of non-uniform temperature field, Int. J. Non-Linear Mech. 99 (2018) 247–257.
[22] M.A. Crisfield, A fast incremental/iterative solution procedure that handles "snap-through", Comput. Struct. 13 (1) (1981) 55–62.
[23] R.T. Haftka, R.H. Mallett, w. Nachbar, Adaption of Koiter's method to finite element analysis of snap-through buckling behavior, Int. J. Solids Struct. 7 (10) (1971) 1427–1445.
[24] C.-Y. Lee, J.-H. Kim, Thermal post-buckling and snap-through instabilities of FGM panels in hypersonic flows, Aerosp. Sci. Technol. 30 (1) (2013) 175–182.
[25] G. Watts, M.K. Singha, S. Pradyumna, Nonlinear bending and snap-through instability analyses of conical shell panels using element free Galerkin method, Thin-Walled Struct. 122 (2018) 452–462.
[26] R. Wiebe, L. Virgin, I. Stanciulescu, S. Spottswood, On snap-through buckling, in: Proceedings of the 52nd AIAA/ASME/ASCE/AHS/ASC Structures, Structural Dynamics and Materials Conference. 2011, American Institute of Aeronautics and Astronautics.
[27] A.M. Dehrouyeh-Semnani, H. Mostafaei, M. Dehrouyeh, M. Nikkhah-Bahrami, Thermal pre- and post-snap-through buckling of a geometrically imperfect doubly-clamped microbeam made of temperature-dependent functionally graded materials, Compos. Struct. 170 (2017) 122–134.
[28] B. Wang, K.S. Fancey, A bistable morphing composite using viscoelastically generated prestress, Mater. Lett. 158 (2015) 108–110.
[29] B. Wang, C. Ge, K.S. Fancey, Snap-through behaviour of a bistable structure based on viscoelastically generated prestress, Compos. Part B: Eng. 114 (2017) 23–33.
[30] N.C. Huang, B. Vahidi, Snap-through buckling of two simple structures, Int. J. Non-Linear Mech. 6 (3) (1971) 295–310.
[31] Y. Chandra, R. Wiebe, I. Stanciulescu, L.N. Virgin, S.M. Spottswood, T.G. Eason, Characterizing dynamic transitions associated with snap-through of clamped shallow arches, J. Sound Vib. 332 (22) (2013) 5837–5855.
[32] M.M. Keleshteri, H. Asadi, Q. Wang, On the snap-through instability of post-buckled FG-CNTRC rectangular plates with integrated piezoelectric layers, Comput. Methods Appl. Mech. Eng. 331 (2018) 53–71.
[33] Y. Chandra, I. Stanciulescu, T. Eason, M. Spottswood, Numerical pathologies in

snap-through simulations, Eng. Struct. 34 (2012) 495–504.
[34] R.H. Plaut, L.N. Virgin, Snap-through under unilateral displacement control with constant velocity, Int. J. Non-Linear Mech. 94 (2017) 292–299.
[35] R.H. Plaut, Snap-through of arches and buckled beams under unilateral displacement control, Int. J. Solids Struct. 63 (2015) 109–113.
[36] L. Liu, B. Lv, T. He, The stochastic dynamic snap-through response of thermally buckled composite panels, Compos. Struct. 131 (2015) 344–355.
[37] J.-S. Chen, S.-Y. Hung, Snapping of an elastica under various loading mechanisms, Eur. J. Mech. - A/Solids 30 (4) (2011) 525–531.
[38] M. Doddamani, V.C. Kishore, N. Shunmugasamy, Gupta, H.B. Vijayakumar, Compressive and flexural properties of functionally graded fly ash cenosphere–epoxy resin syntactic foams, Polym. Compos. 36 (4) (2015) 685–693.
[39] K. Shahapurkar, C.D. Garcia, M. Doddamani, G.C. Mohan Kumar, P. Prabhakar, Compressive behavior of cenosphere/epoxy syntactic foams in arctic conditions, Compos. Part B: Eng. 135 (2018) 253–262.
[40] B.R. Bharath Kumar, M. Doddamani, S.E. Zeltmann, N. Gupta, Uzma, S. Gurupadu, R.R.N. Sailaja, Effect of particle surface treatment and blending method on flexural properties of injection-molded cenosphere/HDPE syntactic foams, J. Mater. Sci. 51 (8) (2016) 3793–3805.
[41] B.R. Bharath Kumar, S.E. Zeltmann, M. Doddamani, N. Gupta, Uzma, S. Gurupadu, R.R.N. Sailaja, Effect of cenosphere surface treatment and blending method on the tensile properties of thermoplastic matrix syntactic foams, J. Appl. Polym. Sci. 133 (35) (2016) (p. n/a-n/a).
[42] A.K. Singh, B. Patil, N. Hoffmann, B. Saltonstall, M. Doddamani, N. Gupta, Additive manufacturing of syntactic foams: part 1: development, properties, and recycling potential of filaments, JOM 70 (3) (2018) 303–309.
[43] A.K. Singh, B. Saltonstall, B. Patil, N. Hoffmann, M. Doddamani, N. Gupta, Additive manufacturing of syntactic foams: part 2: specimen printing and mechanical property characterization, JOM 70 (3) (2018) 310–314.
[44] G. Tagliavia, M. Porfiri, N. Gupta, Analysis of flexural properties of hollow-particle filled composites, Compos. Part B: Eng. 41 (1) (2010) 86–93.
[45] M. Aureli, M. Porfiri, N. Gupta, Effect of polydispersivity and porosity on the elastic properties of hollow particle filled composites, Mech. Mater. 42 (7) (2010) 726–739.
[46] G. Tagliavia, M. Porfiri, N. Gupta, Analysis of hollow inclusion–matrix debonding in particulate composites, Int. J. Solids Struct. 47 (16) (2010) 2164–2177.
[47] S. Waddar, P. Jeyaraj, M. Doddamani, Influence of axial compressive loads on buckling and free vibration response of surface-modified fly ash cenosphere/epoxy syntactic foams, Journal of Composite Materials, 0(0): p. 0021998317751284.
[48] M. Shariyat, D. Asgari, Nonlinear thermal buckling and postbuckling analyses of imperfect variable thickness temperature-dependent bidirectional functionally graded cylindrical shells, Int. J. Press. Vessels Pip. 111–112 (2013) 310–320.
[49] S.E. Zeltmann, K.A. Prakash, M. Doddamani, N. Gupta, Prediction of modulus at various strain rates from dynamic mechanical analysis data for polymer matrix composites, Compos. Part B: Eng. 120 (Suppl. C) (2017) S27–S34.
[50] R.L. Poveda, N. Gupta, Carbon-nanofiber-reinforced syntactic foams: compressive properties and strain rate sensitivity, JOM 66 (1) (2014) 66–77.